Electronic Supplementary Material (ESI) for Energy & Environmental Science.

Supporting Information

Air-Processable High-Efficiency CISSe Solar Cells from DMF Molecular Solution and Their Application to Perovskite/CISSe Tandems

Yasir Siddique[a,b], Kyungnan Son[a,c], Tanka Raj Rana[a], Syed Dildar Haider Naqvi[a,b], Pham Minh Hoang[a,b], Asmat Ullah[a,b], Huyen Tran[a,b], Sang Min Lee[a], Sungjun Hong[a,b], Seung Kyu Ahn*[a], Inyoung Jeong*[a], SeJin Ahn*[a,b]

[a] Photovoltaics Research Department, Korea Institute of Energy Research (KIER), South Korea.

[b] Department of Renewable Energy Engineering, University of Science and Technology, Daejeon, South Korea.

[c] Graduate School of Energy Science and Technology, Chungnam National University, Daejeon, South Korea.

*Corresponding author: SeJin Ahn (swisstel@kier.re.kr)

Experimental procedure

Materials

DMF (99.8%) was purchased from Sigma–Aldrich. TU (99%) was purchased from Acros. Copper chloride (99.99%) and indium chloride (99.999%) were purchased from Sigma–Aldrich. Selenium in elemental form (99.999%, 3 mm shot) was purchased from Cerac. Except for TU, which was recrystallized 2 times, all other chemicals were used as received.

Molecular Solution Preparation

Molecular ink with a Cu/In ratio = 0.9 was prepared as follows: 1.90 g of TU (recrystallized twice) was dissolved in 5 ml of DMF under stirring until the TU was completely dissolved. Then, 0.393 g of copper chloride was added and stirred until complete dissolution. Finally, 0.974 g of indium chloride was mixed into the solution, and the final mixture was heated at 100 °C until all the metal salts were completely dissolved.

Precursor Deposition and Selenization

The precursor solution was spin-coated at 1500 rpm for 60 seconds onto Mo-coated soda-lime glass (SLG) and then annealed at various temperatures of 210, 230, 280 and 330 °C for 2 min. in air to ensure that the film was completely dried and that the initial Cu-In-S phase was formed by decomposition of TU. This process was repeated 5 times to acquire a sufficient absorber thickness. The precursor film was then selenized for 30 min. at 540 °C in a graphite box under an Ar pressure of 160 Torr. Details of the temperature control and calculation of the partial pressure of Se vapor in the selenization furnace can be found in our previous study. [1] After selenization, etching of the films in 20 wt.% $(NH_4)_2S$ solution was performed for 30 min. to remove secondary phases (Cu_xSe).

Device Fabrication

Solar cells were fabricated according to the conventional architecture of SLG/Mo/CISSe/CdS/i-ZnO/ITO/Al. A 60 nm thick CdS buffer layer was deposited onto the CISSe films via chemical bath deposition. A 50 nm thick i-ZnO layer and 160 nm thick ITO layer were then deposited by using radio-frequency magnetron sputtering. An aluminum grid with a 1 μm thickness was deposited via thermal evaporation as a top contact, and through scribing, a 0.44 cm^2 active area was defined. Finally, a 110 nm antireflective coating of MgF_2 was applied to complete the device fabrication process.

Characterization

The morphology and composition of the films were investigated using high-resolution scanning electron microscopy (HRSEM, XL30SFEG Phillips Co., Holland at 10 kV) and EDS (EDAX Genesis apex, acceleration voltage: 30 kV, collection time: 100 s with a standard-less method), respectively. In EDS analysis, the Cu/In ratio was obtained using films deposited on a Mo substrate, and the S/Se ratio was obtained using films deposited on a glass substrate. (There is no difference in the Cu/In ratio between the films deposited on both Mo and glass substrates.)

For structural information of the precursor films, X-ray diffraction (XRD) using a CuKα radiation source (λ = 1.5406 A^0) was employed. A Raman analysis was performed with a Raman spectrometer (NOST, Korea) to analyze phases in the films with a 0.3 mW, 531 nm excitation laser with a spectral resolution of 0.9–1.1/cm (MRA-10).

Focused ion beam (FIB) sampling was performed by using a single beam focused ion beam (SB-FIB) (FB-2100, Hitachi, Japan.) with a gallium liquid metal ion source having an accelerating voltage from 30 kV to 40 kV. A Mo grid was used for FIB sampling of our films. Field transmission electron microscopy (FE-TEM) (Tecnai G^2 F30 S-Twin, FEI, and Netherlands) was used for elemental line scanning (depth profile) TEM analysis of absorber films, with a TEM resolution of 0.17 mm and a focal length of 2.3 mm.

Low-temperature photoluminescence was measured using a high-resolution Raman/PL system (labRAM HR Evolution Visible-NIR, Horiba, France) at 10 K. A laser diode back-illumination source wavelength of 514 nm was selected for the measurement. An 800 mm focal length achromatic flat field monochromator and a multichannel thermal electric cooled (-70 °C) CCD detector were part of the measuring system. A Linkam Stage (LTS 350) was used to maintain the device temperature for measurement.

The J-V characteristics of the devices were measured using an AAA solar simulator (WXS-155S-L2, WACOM, Japan), illumination AM 1.5 G and a Keithley 2450 (Tektronix, USA) source meter. The light intensity was calibrated using an NREL-certified Si-reference cell by before measurements were taken. The J–V curves were measured using a reverse scan (from a forward bias (1.20 V) to short circuit (0 V)) and a forward scan (from a forward bias (0 V) to short circuit (1.20 V)). The step voltage was fixed at 100 mV. The EQE of the solar cell devices was measured at 0 V with an S-9230 system (SOMA Optics, Inc.).

Temperature-dependent J-V in the dark and under illumination and admittance spectroscopy in the dark were performed with a Keithley 2450 source meter and an Agilent LCR meter (4284A), respectively. A Linkam Stage (LTS 350) was used to maintain the device temperature as per the experimental conditions.

S1. Original IV curves of the best devices processed at different air annealing temperatures and relative change in device parameters

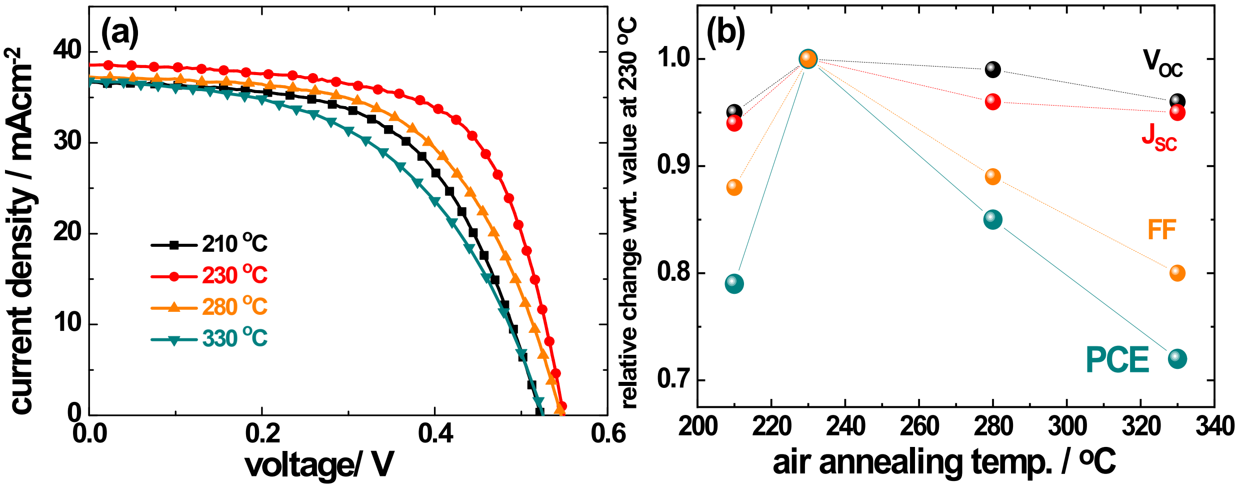

Figure S1. (a) IV curves of best devices processed at different air annealing temperatures of 210, 230, 280 and 330 °C. (b) Relative change in parameters of best devices calculated by normalizing each value with respect to ones at 230 °C condition.

Table S1. Electrical parameters of best devices built with CISSe films processed at different air annealing temperatures of 210, 230, 280 and 330 °C

		V_{oc} / V	J_{sc} / mAcm^{-2}	FF / %	Eff. / %
Air annealing temp. (°C)	210	0.522	36.59	57.80	11.04
	230	0.550	38.56	65.26	13.84
	280	0.546	37.22	58.22	11.83
	330	0.526	36.80	51.70	10.00

S2: Dark IV curves of the devices processed at various air annealing temperatures to extract shunt and series resistance

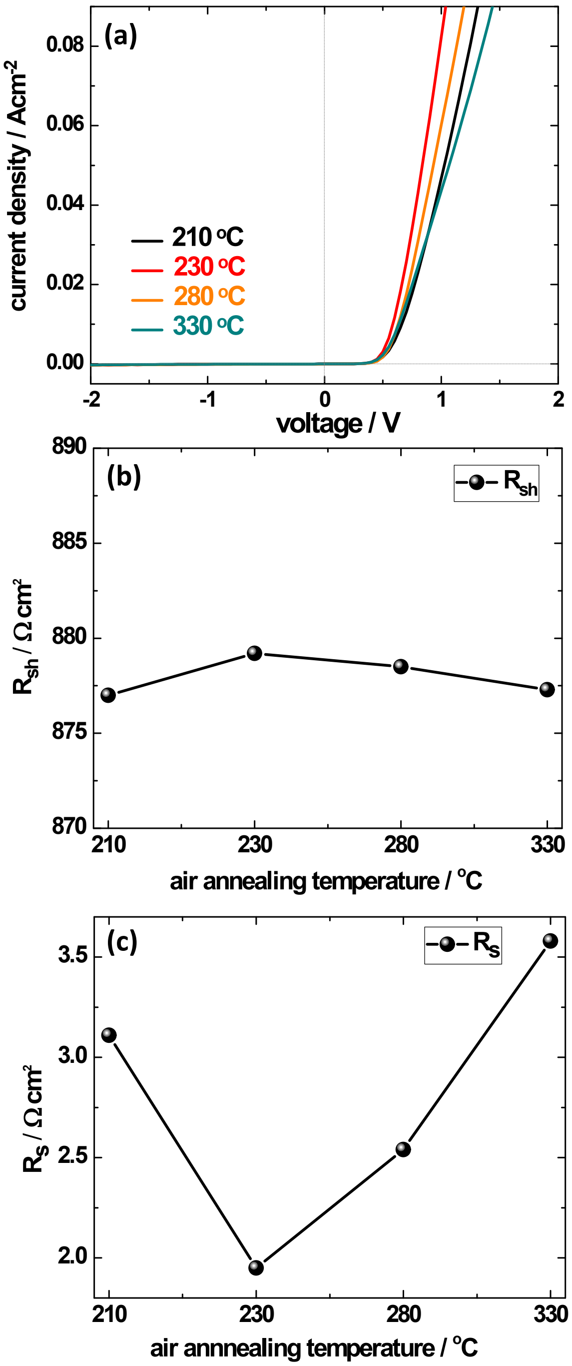

Figure S2. (a) Dark IV curves of best devices processed at different air annealing temperatures of 210, 230, 280 and 330 °C. (b) R_{sh} and (c) R_s extracted from (a).

S3. Surface SEM of CISSe absorbers and cross-sectional SEM and TEM analysis of completed device

(a) Surface SEM of CISSe absorbers

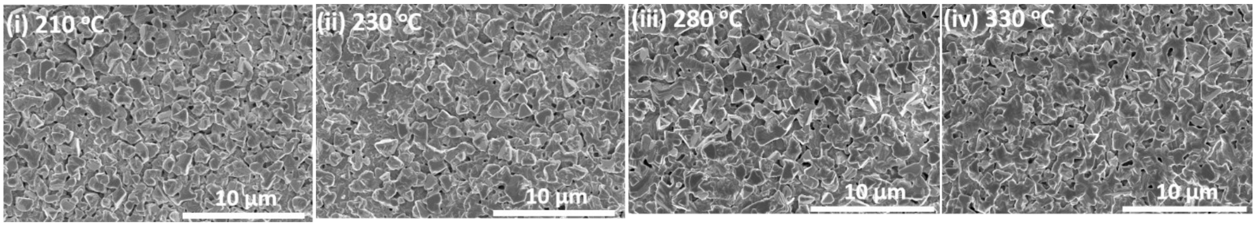

(b) Cross-sectional SEM image and structure of device

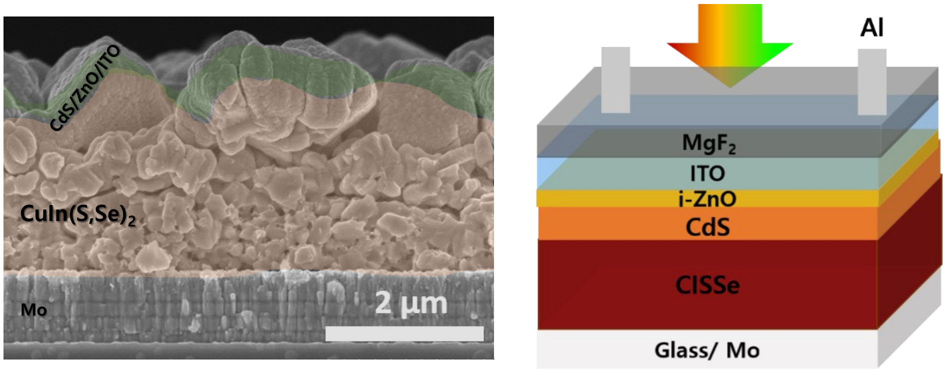

(c) Cross-sectional TEM image and EDS elemental mapping of device

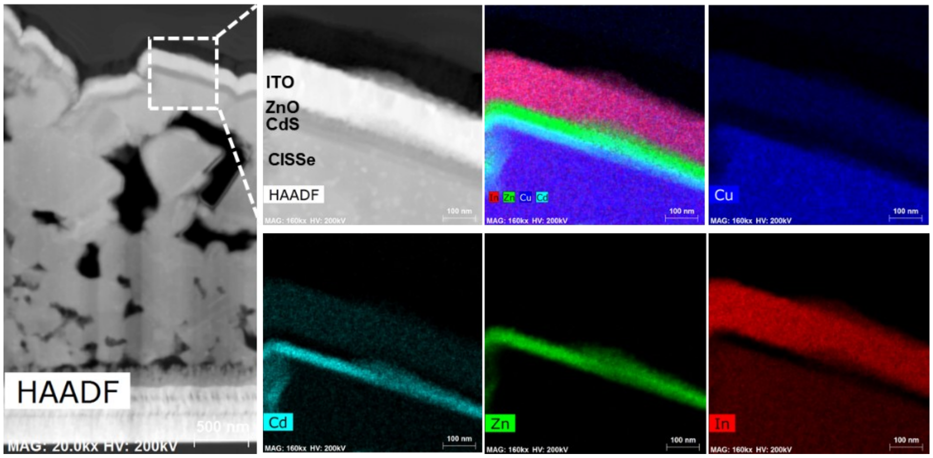

Figure S3. (a) Surface SEM image of CISSe absorbers air-annealed at (i) 210, (ii) 230, (iii) 280 and (iv) 330 °C. (b) Cross-sectional SEM image and structure diagram, and (c) cross-sectional TEM image and EDS elemental mapping of the device built with CISSe film processed at optimum air annealing temperature of 230 °C.

S4: EQE of devices and bandgap calculations

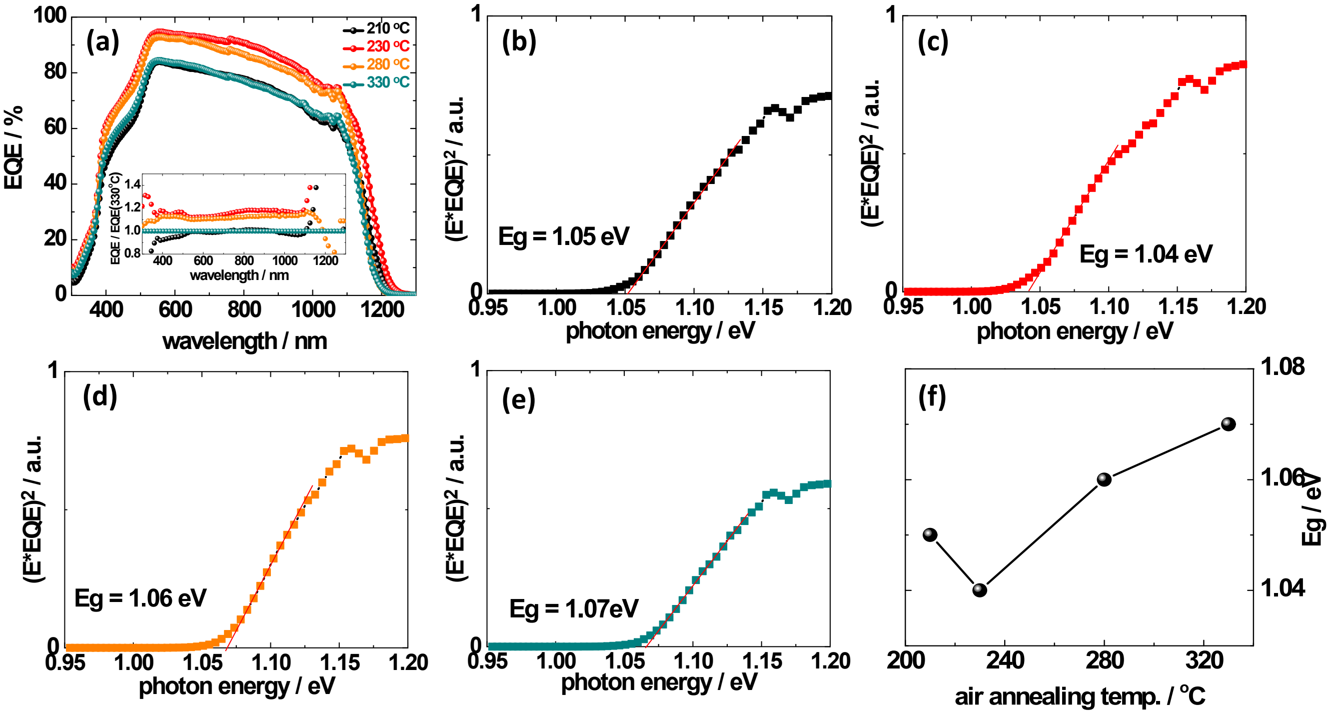

Figure S4. (a) EQE curves of devices. Calculation of bandgap energy (E_g) of CISSe films processed at different air annealing temperatures of (b) 210, (c) 230, (d) 280 and (e) 330 °C. (f) E_g vs. air annealing temperature plot. Inset in (a) shows relative EQE values with respect to 330 °C condition.

S5: Elemental depth profile of CISSe films

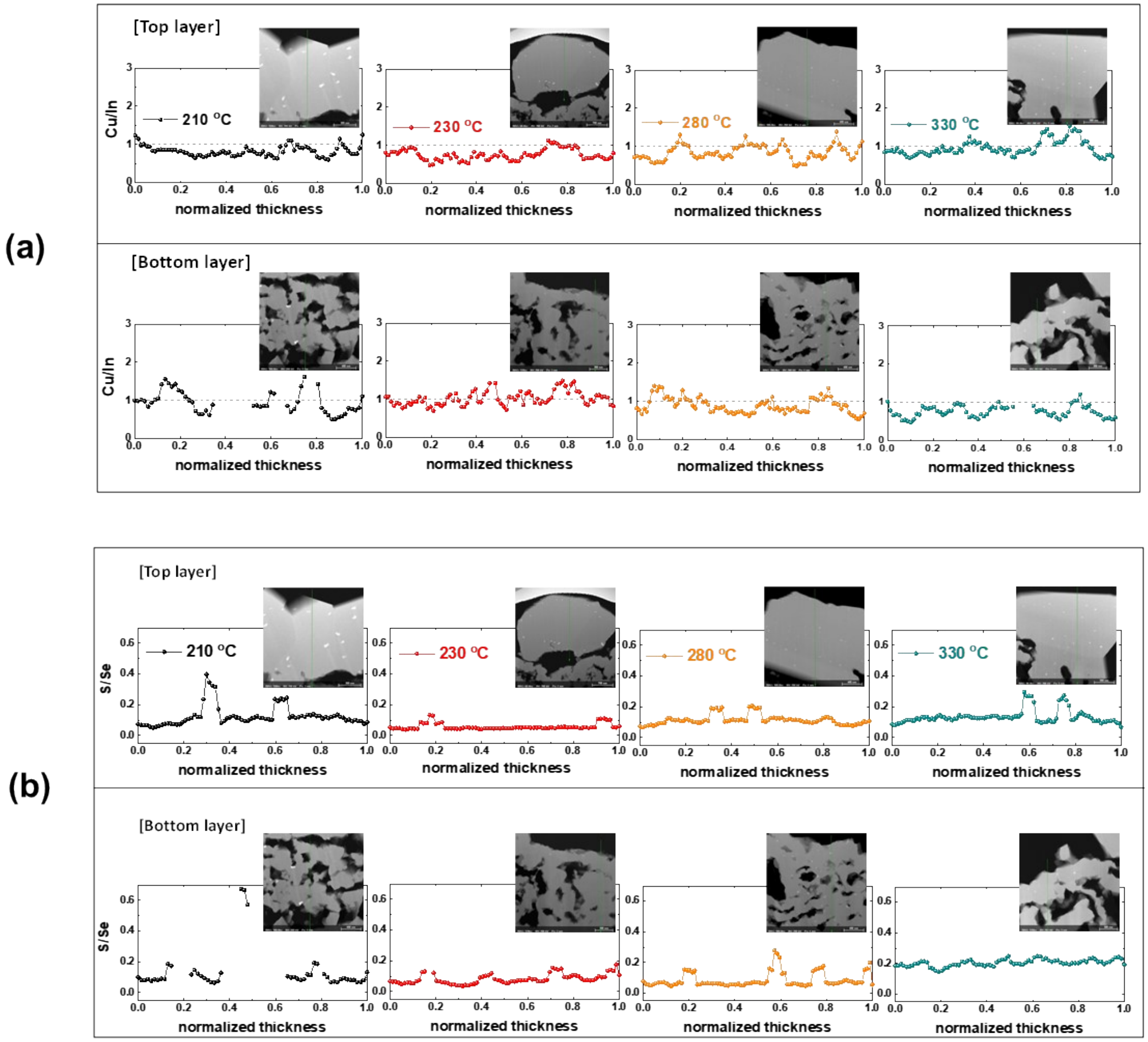

Figure S5. Elemental depth profiles of CISSe films process at different air annealing temperatures obtained by TEM/EDS analysis: (a) Cu/In ratio and (b) S/Se ratio

S6: Temperature dependent admittance spectroscopy

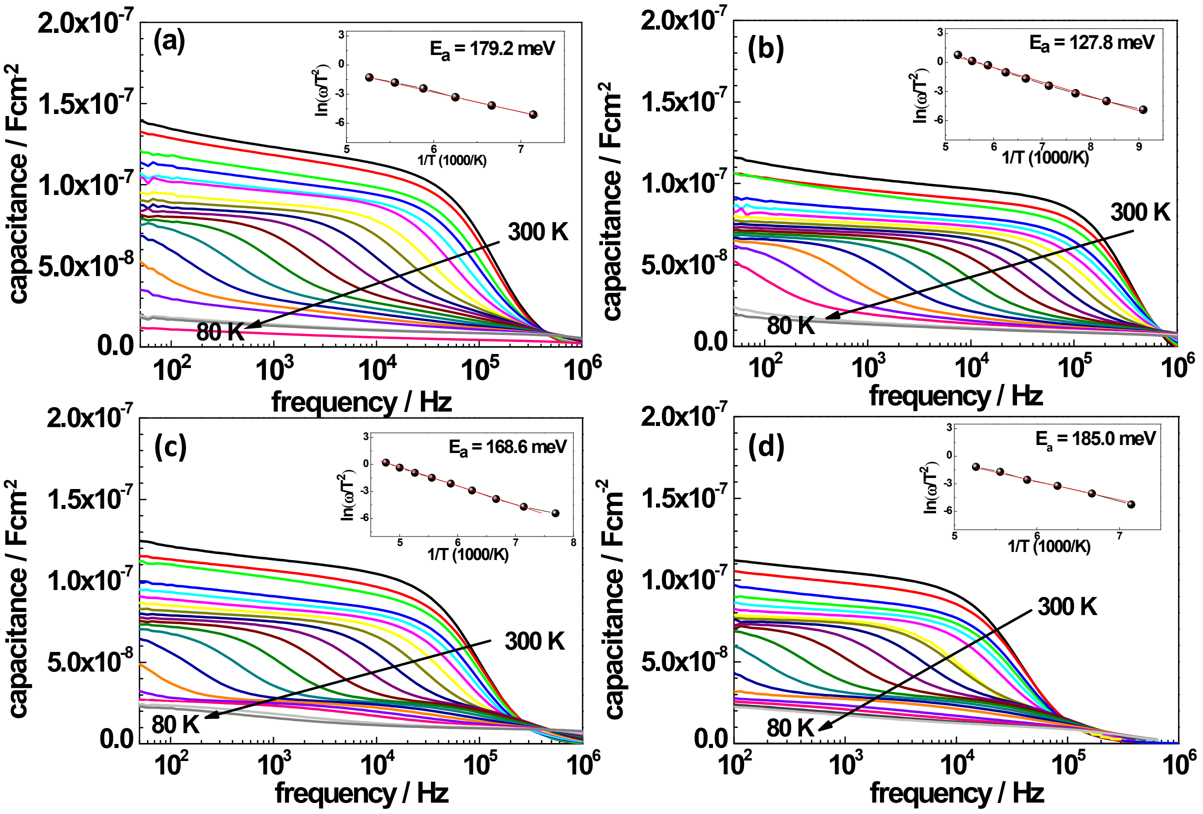

Figure S6. Admittance spectroscopy (AS) data for devices processed at air annealing temperatures of (a) 210, (b) 230, (c) 280 and (d) 330 °C. Insets are ln(ω/T^2) vs. 1/T plots for estimating activation energy.

S7: Defect density calculated from admittance spectra

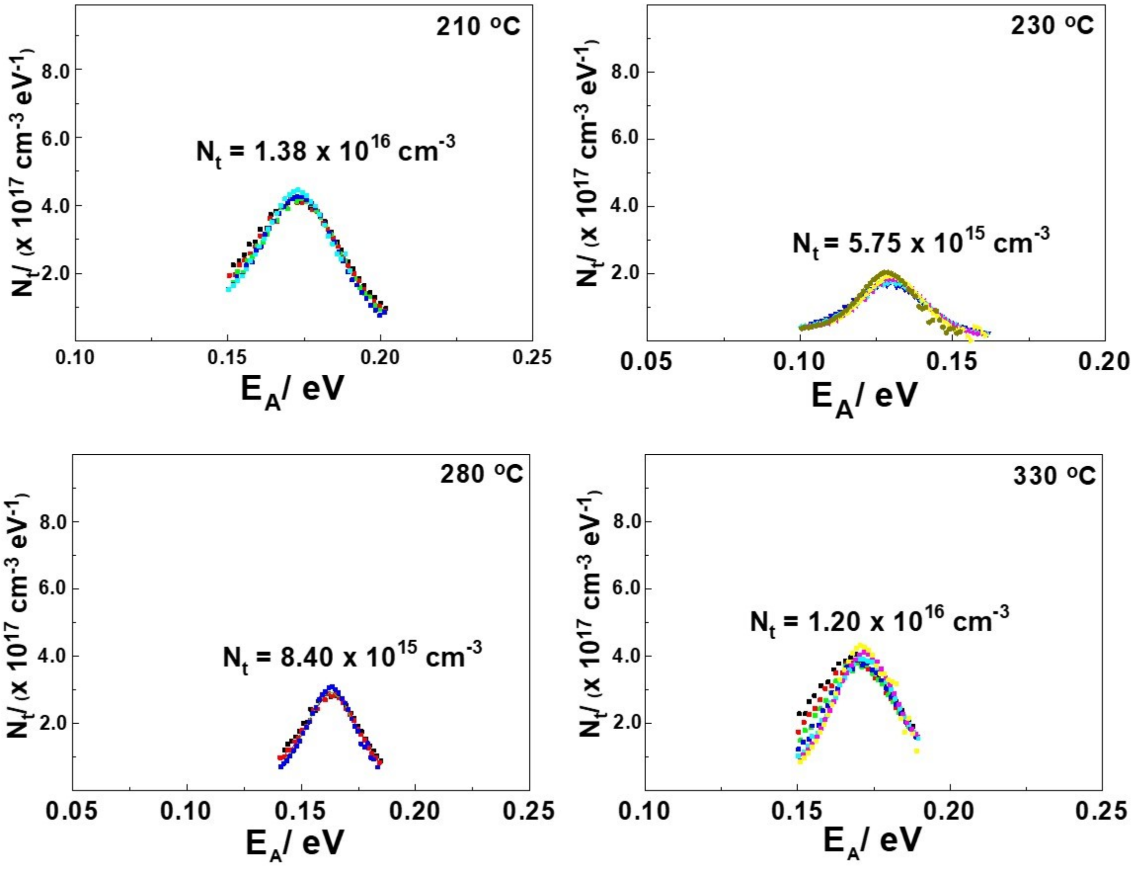

Figure S7. Density of state calculated from Figure S7 for devices processed at different air annealing temperatures.

S8: Raman spectra of unetched CISSe film after selenization

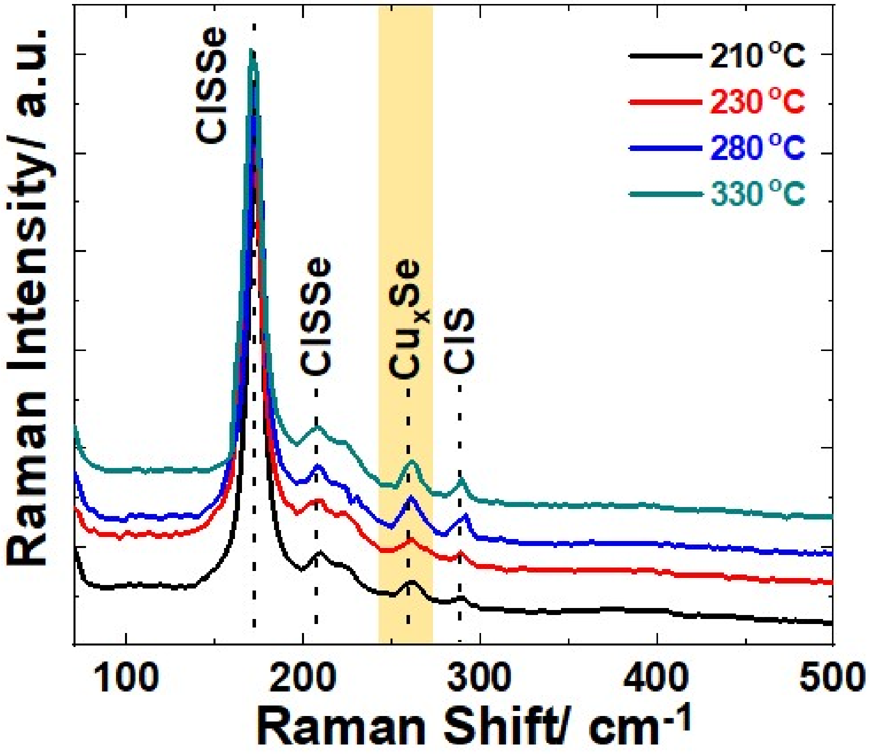

Figure S8. Raman spectra of unetched absorbers films after selenization, processed at different air annealing temperatures.

S9: Growth pathway of CISSe film during selenization

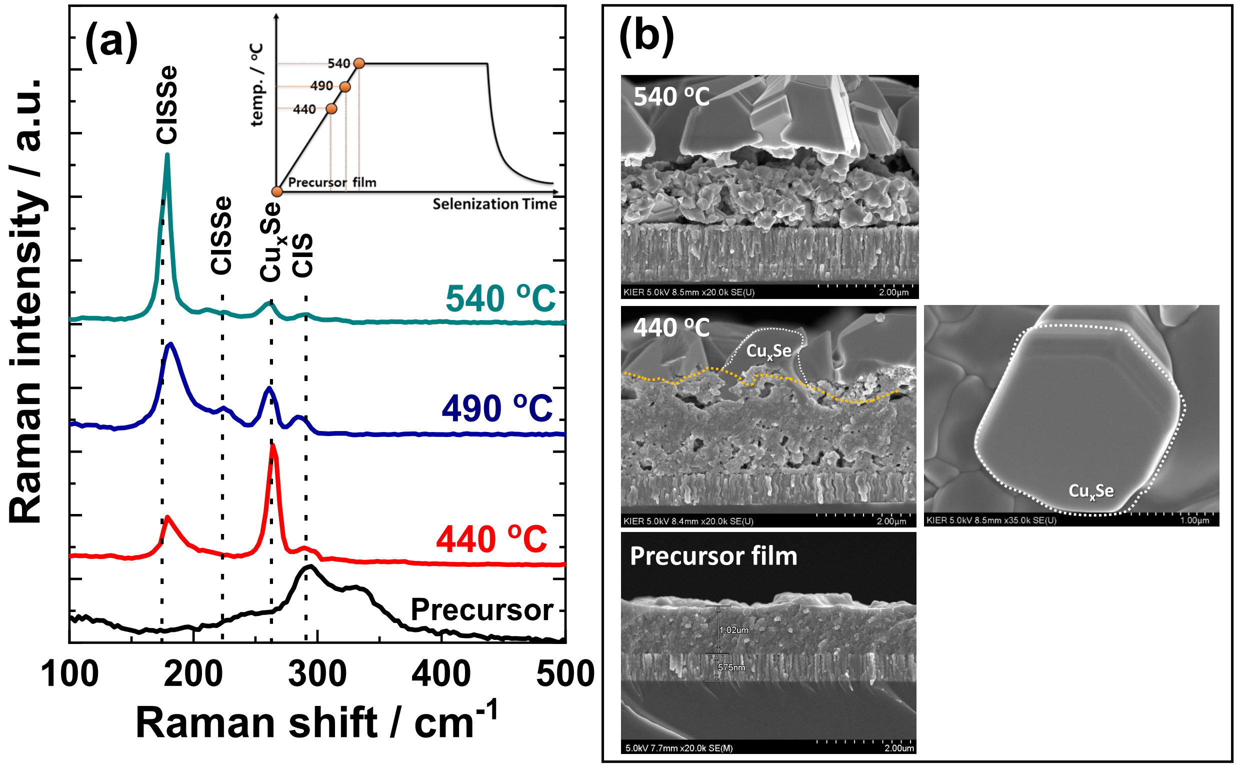

Figure S9: (a) Raman spectra and (b) SEM images of absorber films, processed at air annealing temperature of 210 °C, taken at various steps of selenization shown in inset of (a).

S10: Structural analysis on precursor films during selenization

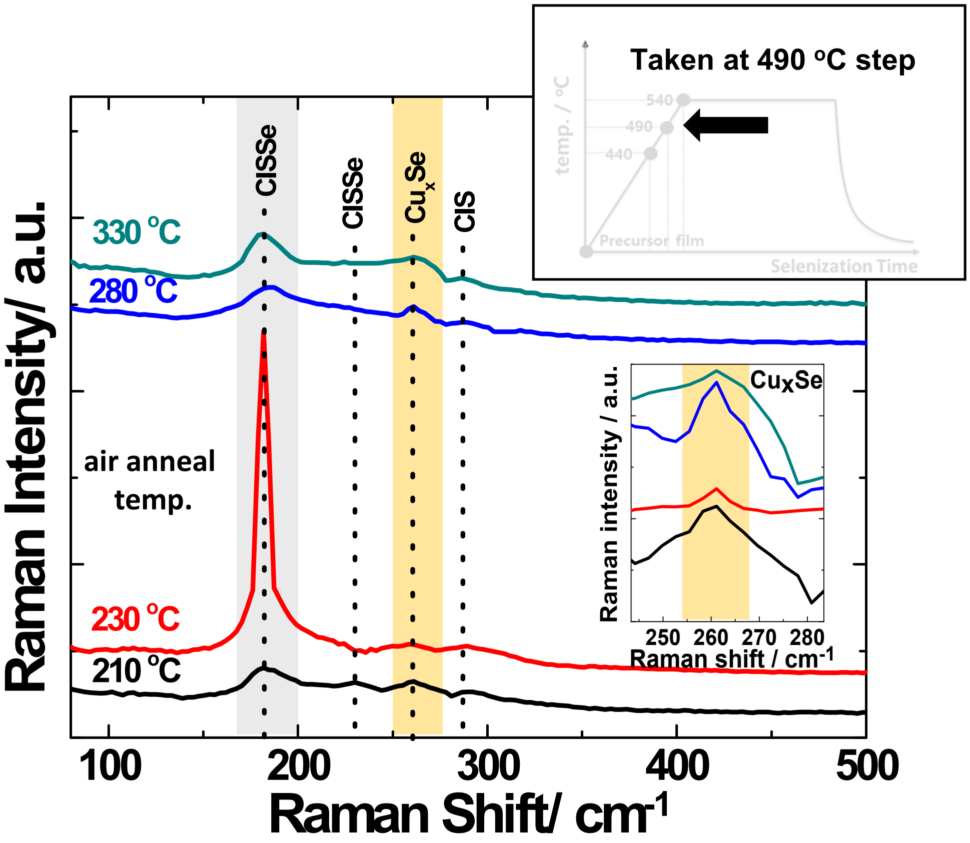

Figure S10. Raman spectra of absorber films, processed at different air annealing temperatures, taken at 490 °C step during selenization in which the exact step is designated in the inset.

S11. Composition characterizations on CISSe films processed at different air annealing temperatures

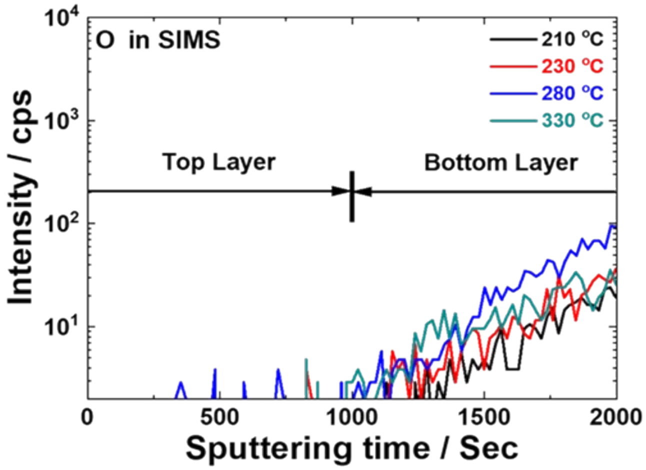

Figure S11. Oxygen depth profile measured from Secondary Ion Mass Spectrometry (SIMS) of the CISSe films processed at different air annealing temperatures.

S12. Certified test result

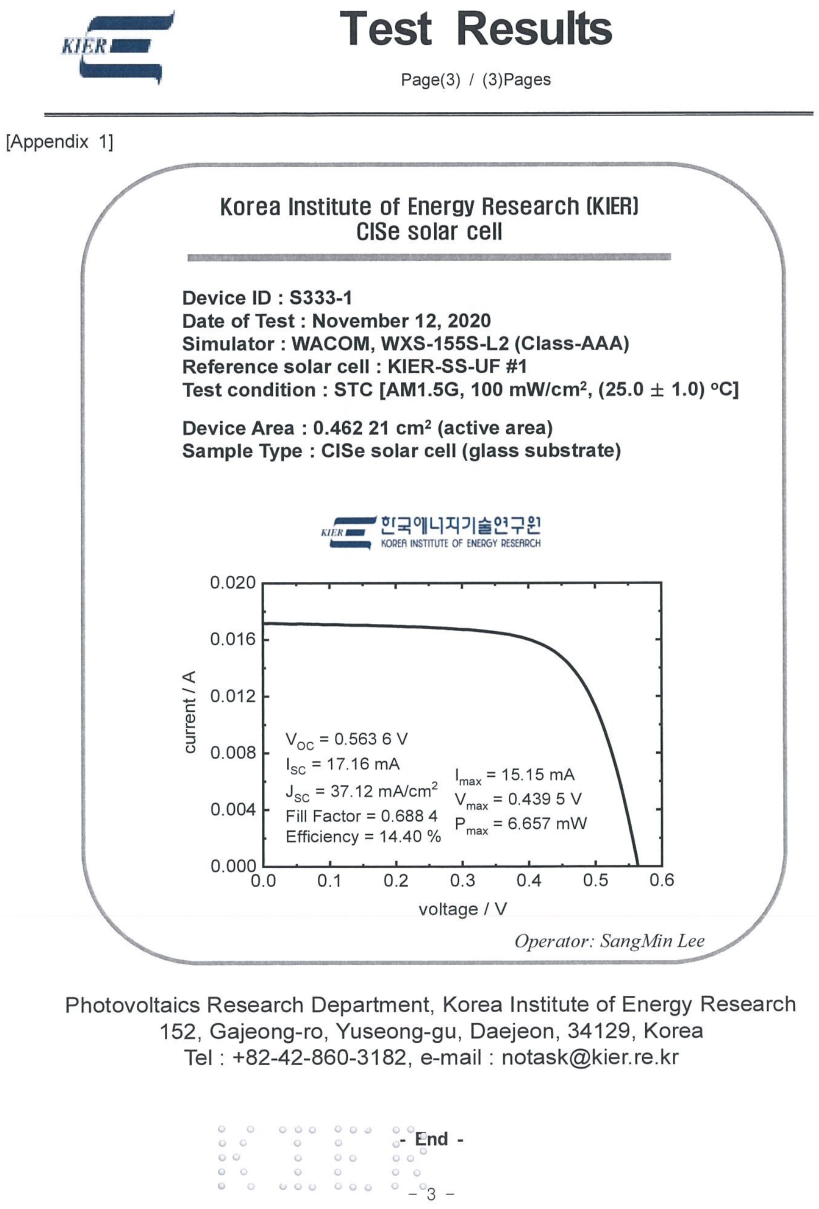

Test Results

Page(3) / (3)Pages

[Appendix 1]

Korea Institute of Energy Research (KIER)
CISe solar cell

Device ID : S333-1
Date of Test : November 12, 2020
Simulator : WACOM, WXS-155S-L2 (Class-AAA)
Reference solar cell : KIER-SS-UF #1
Test condition : STC [AM1.5G, 100 mW/cm², (25.0 ± 1.0) °C]

Device Area : 0.462 21 cm² (active area)
Sample Type : CISe solar cell (glass substrate)

한국에너지기술연구원
KOREA INSTITUTE OF ENERGY RESEARCH

V_{OC} = 0.563 6 V
I_{SC} = 17.16 mA
J_{SC} = 37.12 mA/cm^2
Fill Factor = 0.688 4
Efficiency = 14.40 %

I_{max} = 15.15 mA
V_{max} = 0.439 5 V
P_{max} = 6.657 mW

Operator: SangMin Lee

Photovoltaics Research Department, Korea Institute of Energy Research
152, Gajeong-ro, Yuseong-gu, Daejeon, 34129, Korea
Tel : +82-42-860-3182, e-mail : notask@kier.re.kr

- End -

Figure S12. Certified I-V curve of the best CISSe device

S13. Schematic diagram of the tandem device

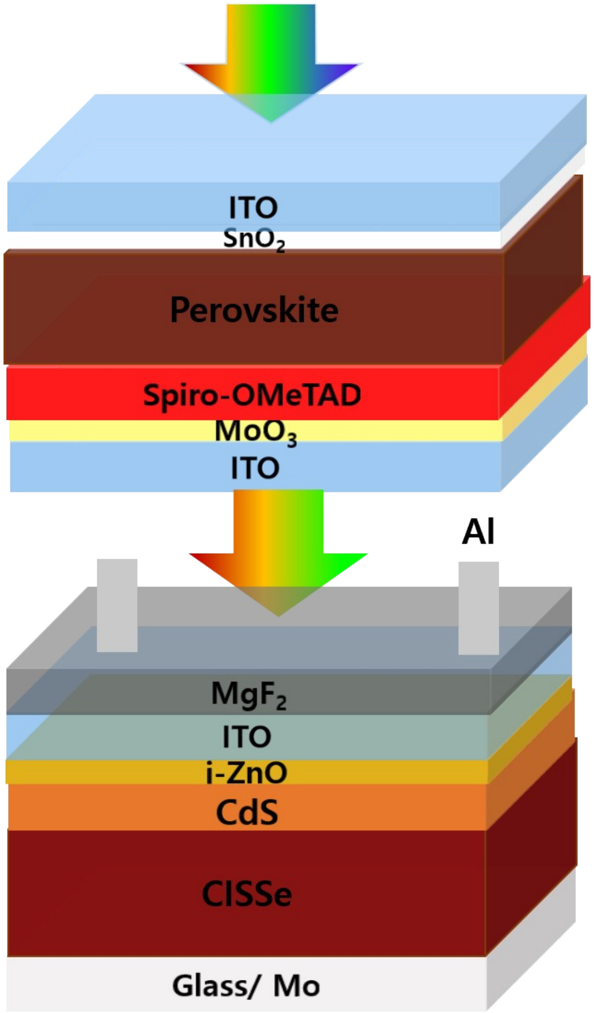

Figure S13. Schematic of the 4-T perovskite/CISSe solar cell

S14. Transmittance data of semitransparent perovskite top cell (without metal grid)

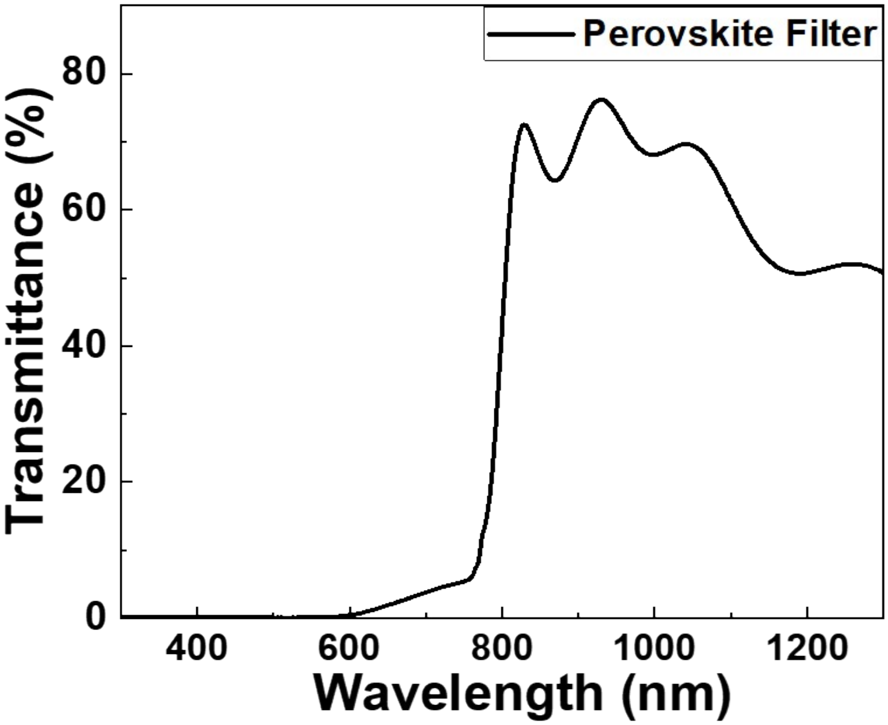

Figure S14. Transmittance of the semitransparent perovskite filter used for 4-T tandem measurements

Procedure of fabrication of Semitransparent Perovskite device

For top cell fabrication, ink preparation has been carried out in N_2 filled glove box with water and oxygen contents below 20 ppm while ink deposition and its drying was done in ambient conditions. For electron transport layer, SnO_2 nanoparticles in DI water at a mass ratio of 1:4 were prepared and stirred for 4 hours. PbI_2 solution was prepared by dissolving 1.5 M PbI_2 in DMF: DMSO (9:1) solvents and it was stirred at 70 ^{o}C for at least 3 hours. Then FAI (450 mg), MAI (32 mg), MACl (45 mg) was added in 5 ml IPA to make organic halide solution. 15 mM OAI solution for surface treatment was used by mixing OAI in IPA. For hole transport layer, Spiro-OMeTAD 72.3mg + CB 1mL + Li-TFSI 35µL (Li-TFSI/ACN=260mg/mL stock solution) + tbp 30µL solution was prepared to make a clear solution.

At first, cleaning of glass/ITO was done by sonication in DI water, acetone and ethanol for 15 min. Then ETL was spin coated at 4000 rpm/ 30 s, and is annealed at 150 ^{o}C for 15 min. Then after filtration, absorber layer was formed by 2-step method in which PbI_2 layer was first deposited by spin coating, followed by (FAI+MAI+MACl) solution deposition at 2000 rpm. The deposited films were annealed at 150 ^{o}C for 15 min. Then dynamic spin coating of OAI solution was done for surface treatment at 3000 rpm. Afterwards, Spiro-OMeTAD solution was spin coated at 1500 rpm for 30 sec. Then, MoO_x (20 nm) buffer layer was thermally evaporated on the sample. After it, ITO (200 nm) was deposited as transparent conducting oxide layer by sputtering. Finally, ~ 80 nm Au electrode was deposited at the edge region of ITO layer to improve contact property during measurement by using thermal evaporator to complete the device.

References:

1. Han, J.H., Rehan, S., Moon, D.G., Cho, A., Gwak, J., Yoon, K.H., Ahn, S.K., Yun, J.H., Eo, Y.J., and Ahn, S., *Journal of Materials Chemistry A*, 2016, **4**, 6319–6331.
2. Zahedi-Azad, S., Maiberg, M., and Scheer, R., *Progress in Photovoltaics: Research and Applications*, 2020, **28**, 1146-1157.
3. Werner, F., Wolter, M.H., Siebentritt, S., Sozzi, G., Napoli, S. D, Menozzi, R., Jackson, P., Witte, W., Carron, R., Avancini, E., Weiss T.P., Buecheler S., *Progress in Photovoltaics: Research and Applications*, 2018, **26**, 911–923.